Journal of Alloys and Compounds 509 (2011) 5926–5930

Contents lists available at ScienceDirect

Journal of Alloys and Compounds

journal homepage: www.elsevier.com/locate/jallcom

Characterization of the surface film on Zr-based bulk metallic glass using X-ray photoelectron spectroscopy (XPS) and scanning electron microscopy (SEM)

Ming Tan*, Qiao Liu, Nian Zhang, Huiqin Hu, Biao Li, Xianjie Kang

College of Physical Science and Technology, Central China Normal University, Wuhan 430079, China

ARTICLE INFO

Article history:
Received 16 February 2011
Accepted 6 March 2011
Available online 12 March 2011

Keywords:
Zr-based metallic glass
XPS
SEM
Passive films

ABSTRACT

Using XPS, we have for the first time studied the release of metal ions in the film of the Zr-based bulk metallic glass to the corrosive solutions during immersing. The composition of Al ions in the film of the as-cast metallic glass (41%) is substantially higher than the nominal Al composition of the alloy (9.5%). We proposed that the enriched Al ions can be attributed to the preferential oxidation of Al atoms. After immersing in the NaCl- and HCl-solution, the composition of Al ions in the films decreases from 41% to 28.09% and 21.76%, respectively. This indicates that some of the Al ions in the film are dissolved into the solution during immersion. The composition changes of metal ions in the film of the immersed alloys relative to those of the as-cast metallic glass were discussed using the point defect model. SEM was also used to examine the surface morphology of the samples. No pit corrosion was observed in the SEM images of the immersed metal glass.

1. Introduction

Metallic glasses do not have crystal defects like grain boundaries and dislocations and are chemically homogeneous single-phase alloys. Such structure character allows metallic glasses to possess unique physical, chemical and mechanical properties. Early prepared metallic glasses are in the form of ribbon with thickness smaller than 100 μm and this limits applications of this new type alloy [1]. Since the discovery of the alloy systems for which large size bulk metallic glasses can be prepared using conventional metal processing such as casting [2–5], bulk metallic glasses have attracted much attention. A review on bulk metallic glasses has been given by Wang et al. [6]. Bulk metallic glasses can find various applications [6]. For example, Zr-based bulk metallic glasses have demonstrated a promising potential for biomedical applications since they have very good mechanical properties [7,8] and excellent corrosion resistance [9], biocompatibility [10–12].

When an (amorphous or crystalline) alloy is exposed to air, an oxidation film with a thickness of several nanometers will form on the surface of the alloy very soon [13,14]. Implanting the alloy into the human body, the surface film on the alloy is attacked by Cl^- ions in the body fluid. Such attacks can cause some of the metal ions in the film to dissolve into the body fluid. Ions of some metal elements (say Al) are harmful to the human body. Therefore, we wish to understand what metal ions in the film of a biomaterial are dissolved into the body fluid. However, no such studies have been undertaken on the biomaterial – the $Zr_{60.5}Cu_{19.5}Ti_{5.5}Al_{9.5}Fe_5$ bulk metallic glass. The aim of this paper is to investigate what metal ions are dissolved into the corrosive solution when the $Zr_{60.5}Cu_{19.5}Ti_{5.5}Al_{9.5}Fe_5$ bulk metallic glass is immersed.

2. Experimental procedure

An alloy ingot with the nominal composition of $Zr_{60.5}Cu_{19.5}Ti_{5.5}Al_{9.5}Fe_5$ was prepared by arc-melting the mixture of pure Zr, Cu, Ti, Fe, and Al metals with purity better than 99.5% in an argon atmosphere. A bulk metallic glass (BMG) cylindrical rod of 3 mm diameter was produced by copper mould casting from the master alloy. To prepare samples for the XPS and SEM experiments, an as-cast rod was first cut into slices with thickness of 2–3 mm. The slices were then thinned mechanically with SiC papers from grit 320 to grit 2000. The thickness of the samples for XPS and SEM measurements was around 1.5 mm.

These slices were examined by X-ray diffraction using a Dandong diffractometer (XRD, Y-2000) with CuKα radiation. The thermal analysis was also performed at a heating rate of 20 °C/min in an argon atmosphere using differential scanning calorimetry (DSC, PerkinElmer DSC-7).

XPS measurements were performed using a Thermo VG Scientific VG Multilab 2000 photoelectron spectrometer with monochromatized Al Kα excitation. We performed XPS measurements on three samples. Sample 1 was the as-cast metallic glass. Sample 2 was the NaCl solution immersed metallic glass. The as-cast metallic glass sample was immersed in a 0.13 M NaCl solution (which is the NaCl concentration in the human body fluid) for 168 h. Sample 3 was the HCl solution immersed metallic glass. The as-cast metallic glass sample was immersed in a 1 M HCl solution for 168 h. Prior to immersion and XPS measurements, all the samples were washed with ethanol and distilled water in an ultrasonic bath. The surface examination was performed using field-emission scanning electron microscopy (FE-SEM, JEOL–6700F).

* Corresponding author.
E-mail address: tanming@phy.ccnu.edu.cn (M. Tan).

0925-8388/$ – see front matter © 2011 Elsevier B.V. All rights reserved.
doi:10.1016/j.jallcom.2011.03.051

3. Results

Fig. 1 gives the XRD pattern of the as-cast $Zr_{60.5}Cu_{19.5}Al_{9.5}Ti_{5.5}Fe_5$ bulk alloy. There is a diffused diffraction peak in the XRD pattern. Fig. 2 shows the DSC curve measured at a heating rate of 20 °C/s. Two exothermal peaks were observed. The results of XRD and DSC indicate that this bulk alloy is an amorphous alloy.

Fig. 3 shows an overall XPS spectrum of the as-cast metallic glass sample. We observed the peaks of Al 2p, Zr 3d 3p, C 1s, Ti 2p, Cu 2p, O 1s, etc. The C 1s peak located at around 285.0 eV is attributed to a contaminant hydrocarbon layer, which covered the topmost surface of the sample. These carbon-based contaminants can originate from exposure of the sample to mechanical-pumping oil (during XPS experiments). The O 1s spectrum, shown in Fig. 4, consists of two overlapping peaks. The peak at 531.8 eV is attributed to OH oxygen, which is OH^- ions and water molecules adsorbed on the surface. OH^- ions and water molecules, which originate from exposure of the sample to air, also covered the topmost surface of the sample. The peak at 529.7 eV is due to OM oxygen, which is due to O^{2-} ions in the metal oxides. The peaks due to carbon-based contaminants (C 1s), OH and OM oxygen (O 1s) were observed in all the samples.

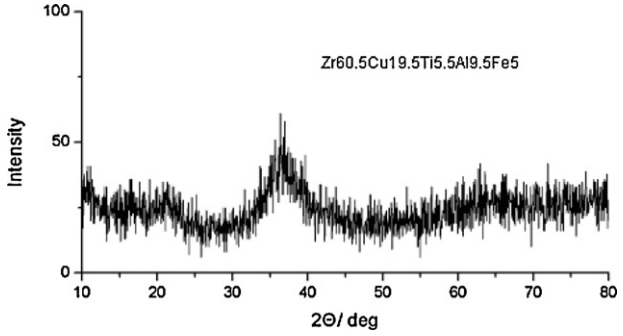

Fig. 1. An X-ray diffraction pattern of the as-cast metallic glass $Zr_{60.5}Cu_{19.5}Ti_{5.5}Al_{9.5}Fe_5$.

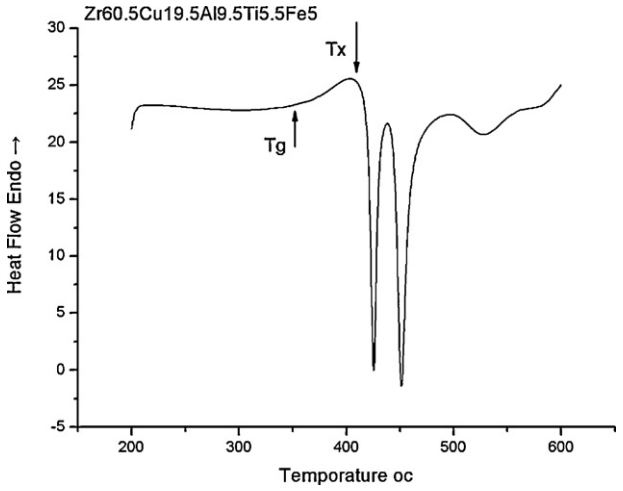

Fig. 2. The DSC curve of the as-cast metallic glass, which was obtained at a heating rate of 20 °C/s. The crystallization temperature (T_x) is around 400 °C. The exothermal peak ends at a temperature of around 470 °C.

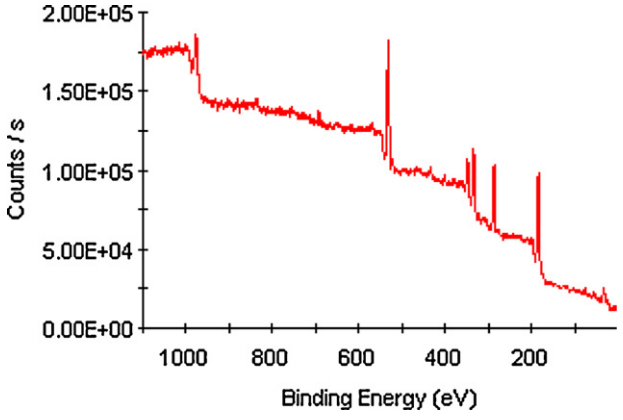

Fig. 3. An overall XPS spectrum of the as-cast metallic glass alloy.

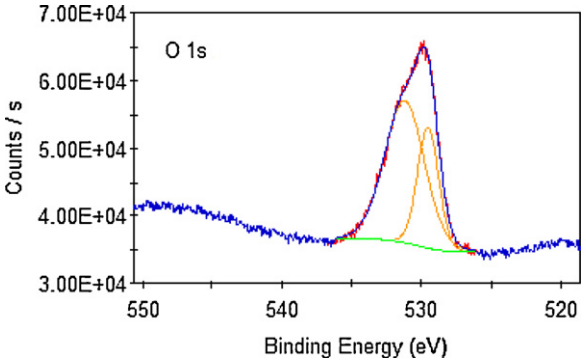

Fig. 4. The experimental and fitted XPS spectrum of O 1s of the as-cast sample. This spectrum is divided into two overlapping peaks. The peak at 531.8 eV is attributed to OH oxygen, which is OH^- ions and water molecules adsorbed on the surface. The peak at 529.7 eV is due to OM oxygen, which is due to O^{2-} ions in the metal oxides.

Fig. 5(a–e) give the spectrum of Al 2p, Zr 3d, Ti 2p, Cu 2p and Fe 2p electrons of the as-cast metallic glass sample, respectively. The peak of Al 2p (Fig. 5a) appears at 70–80 eV and is due to Al 2p electrons of Al^{3+} ions. The spectrum of Zr 3d electron (Fig. 5b) is a doublet of the Zr $3d_{5/2}$ and $3d_{3/2}$ peaks from the Zr^{4+} state, which are at 183.0 and 185.3 eV, respectively. The spectrum of Ti 2p electron (Fig. 5c) is a doublet of the Ti $2p_{3/2}$ and $2p_{1/2}$ peaks from the Ti^{4+} state, which appears at 458 and 464 eV, respectively. The spectrum of Cu 2p electron (Fig. 5d) is also a doublet of the Cu $2p_{3/2}$ and $2p_{1/2}$ peaks from the Cu^{2+} state, which appears at 931 and 953 eV. No ions of Fe were detected (Fig. 5e). The compositions of metal ions in the film of the as-cast sample have been determined and are given in Table 1. In Table 1, peaks of C 1s and O 1s are excluded from the composition.

The XPS peaks of the other two samples have the same positions as those of the as-cast sample, indicating that the oxidation states of the metal atoms of the film are the same in all the samples. The composition data of these two samples are also aggregated in Table 1. It is seen from Table 1 that the compositions of metal ions in the film of the as-cast sample are different from the nominal compositions of the alloy. The metal ion compositions of the films of the three samples are different from each other. No ions of Fe were detected in the film of all the samples. Compared with the nominal compositions of the alloy, the composition of Cu in the film of the as-cast

Table 1
The composition of metal ions in the film of three samples. The first sample is the as-cast metallic glass $Zr_{60.5}Cu_{19.5}Ti_{5.5}Al_{9.5}Fe_5$. The second one is the NaCl solution immersed metallic glass. The third one is the HCl solution immersed metallic glass. Peaks of C 1s and O 1s are excluded from calculation of the atomic composition.

	Sample 1	Sample 2	Sample 3
Zr (at.%)	51.58	68.3	69.02
Cu (at.%)	2.85	2.92	4.48
Ti (at.%)	4.28	0.7	4.74
Al (at.%)	41.29	28.09	21.76

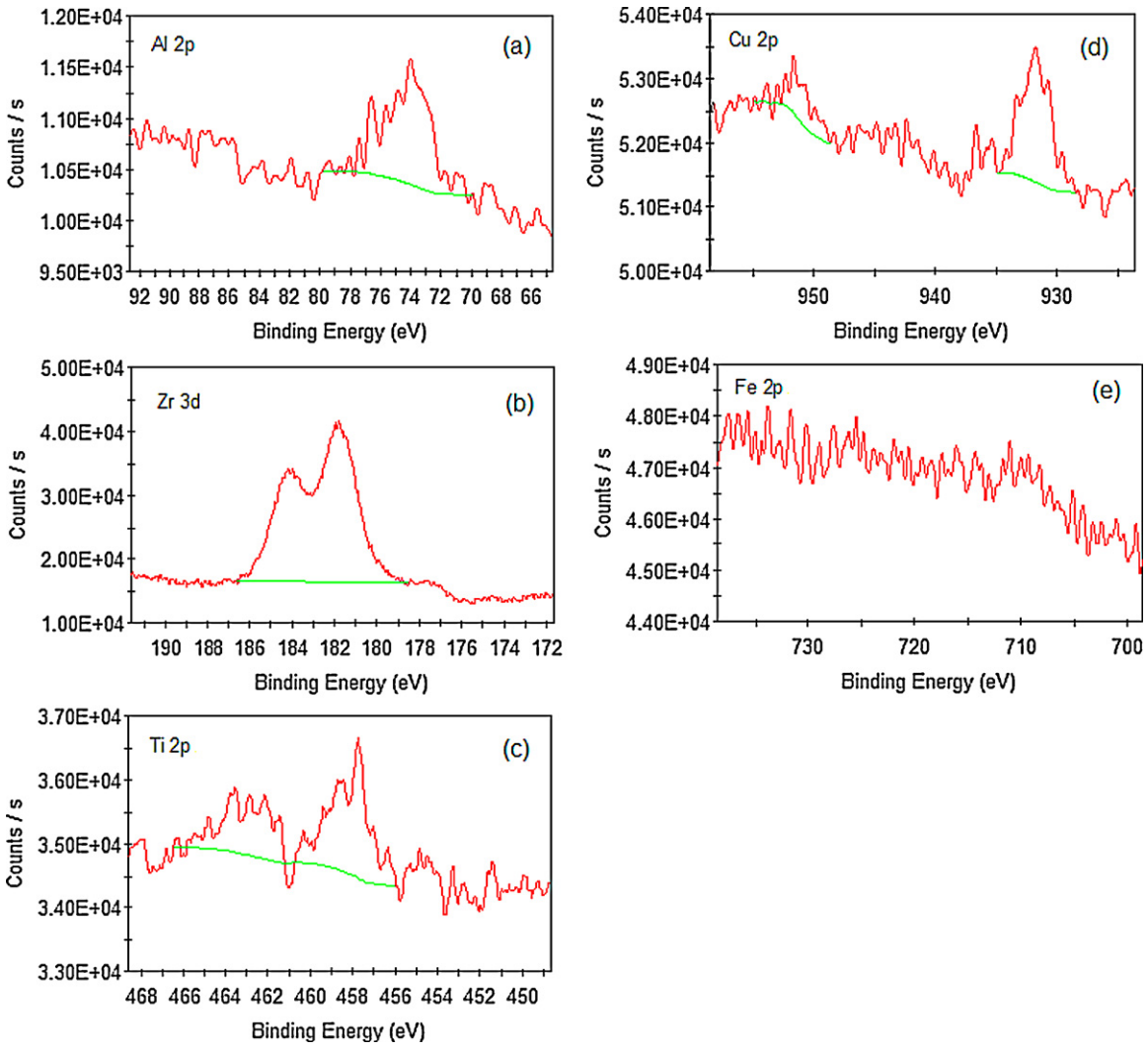

Fig. 5. The experimental XPS spectra of metal ions in the surface film of the as-cast sample: (a) Al 2p electrons of Al^{3+} ions; (b) Zr 3d electrons, a doublet of the Zr $3d_{5/2}$ (183.0 eV) and $3d_{3/2}$ (185.3 eV) peaks from the Zr^{4+} state; (c) Ti 2p electrons, a doublet of the Ti $2p_{3/2}$ (458 eV) and $2p_{1/2}$ (464 eV) peaks from the Ti^{4+} state; (d) Cu 2p electrons, a doublet of the Cu $2p_{3/2}$ (931 eV) and $2p_{1/2}$ (953 eV) peaks from the Cu^{2+} state; (e) Fe 2p electrons, there are little of Fe ions in the film.

sample decreases significantly and the composition of Al increases very much. After immersion in the NaCl- and HCl-solutions, the composition of Al ions in the film decreases substantially.

We used a field-emission scanning electron microscopy (FE-SEM) to examine the surface morphology of all the samples. Fig. 6 shows the FE-SEM images of the as-cast metallic glass (Fig. 6a), the NaCl- (Fig. 6b) and HCl- (Fig. 6c) solution immersed metallic glass. It can be seen from Fig. 6 that no pit corrosion occurs.

4. Discussion

Putting the metal (or an alloy) into a NaCl- (or HCl-) solution, corrosion reactions will occurs. According the point defect model, there are two reactions at the metal/film interface and three reactions at the film/solution [13]. The two reactions at the metal/film interface are

$$m + V_M^{\chi'} \rightarrow M_M + V_m + \chi e' \quad (1)$$

$$m \rightarrow M_M + (\tfrac{\chi}{2})V_{\ddot{O}} + \chi e' \quad (2)$$

The three reactions at the film/solution interface are expressed by

$$M_M \rightarrow M^{\delta+}(aq.) + V_M^{\chi'} + (\delta - \chi)e' \quad (3)$$

$$V_{\ddot{O}} + H_2O \rightarrow O_O + 2H^+ \quad (4)$$

$$MO_{\chi/2} + \chi H^+ \rightarrow M^{\delta+} + \frac{1}{2}H_2O + (\delta - \chi)e' \quad (5)$$

where m denotes a metal atom, $V_M^{\chi'}$ a cation vacancy, M_M a metal cation in a cation site, V_m a vacancy in metal phase, $V_{\ddot{O}}$ an anion vacancy, O_O an oxygen ion in anion site. In reaction (2), a new film $(M_M + (\chi/2)V_{\ddot{O}})$ is produced. Reaction (3) causes metal cations to leave the film surface and to dissolve into solution. In reaction (5), film $(MO_{\chi/2})$ is destructed and dissolved into solution. Reactions (3) and (5) cause the metal ions in the film to release into solution, thus leading to the composition change of metal ions in the film. Therefore, we believe that the composition changes of metal ions in the film carry information on the transportation of metal ions through the film and on the dissolution of the film and the metal ions in the film into solution. Moreover, if the rate of reaction (2) is the same as that of reaction (5), the steady state corrosion occurs (that is, the new produced film is equal in quantity to the film dissolved into solution [13].

In the following, we discuss results of SEM and XPS using the point defect model and attempt to elucidate three questions by this discussion. The first question is on the transportation of metal ions through the film. The second question is on the dissolution

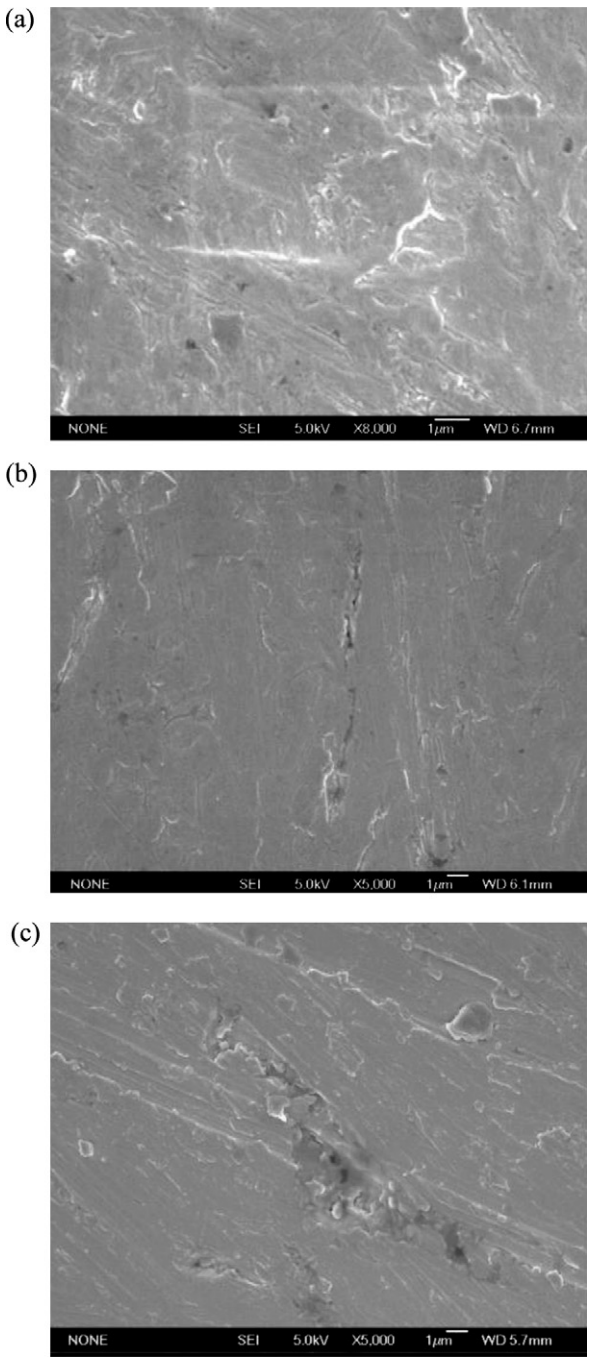

Fig. 6. The SEM images of three samples: the as-cast metallic glass (a), the NaCl- (b) and HCl- (c) solution immersed metallic glass.

of the film into solution. The third question is what metal ions are dissolved into solution. First of all, we explain the composition changes of metal ions in the film of the as-cast metallic glass with respect to the nominal composition of the alloy. Then the composition changes of the metal ions of the immersed metallic glass relative to the as-cast metallic glass are discussed.

4.1. Composition changes of metal ions in the film of the as-cast metallic glass relative to the nominal composition of the alloy

The nominal composition of the alloy can be regarded as the atomic composition inside the bulk alloy. The nominal composition is different significantly from the composition of metal ions in the film of the as-cast sample, as shown in Table 1. We can see from Table 1 that the composition of Al ions (41.3%) is much higher than the nominal Al composition of the alloy (9.5%). The composition of Ti ions (4.2%) is almost equal to the nominal composition (5.5%). The composition of metal ions of Zr, Cu and Fe are lower than the nominal concentration of the alloy. We suggest that the composition changes should be explained in terms of the preferential oxidation of metal atoms, which occurred in the film when the sample was exposed to air.

Using the pure Ni metal and NiAl alloy as an example, we first argued that the preferentiality of oxidation of a metal atom in an alloy can be mainly determined by the Standard Electrode Potential. The Standard Electrode Potentials [15], which is measured relative to the standard oxidation of hydrogen gas, measures the ability of the metal atoms to get oxidized (i.e., give up its electrons). The lower the Standard Electrode Potentials, the easier the oxidization reaction. The Standard Electrode Potential is −1.66 V for the reaction $Al^{3+} + 3e^- \leftrightarrow Al(s)$ [16], and −0.25 V for the reaction $Ni^{2+} + 2e^- \leftrightarrow Ni(s)$ where (s) represents solid. Tan and King have studied the population, angular and time-of-flight mass spectra of Al and Ni neutral atoms sputtered from the surfaces of Ni(1 0 0) and NiAl(1 1 0) single crystals under a ultra high vacuum (UHV, the base pressure of chamber is 1.5×10^{-9} mbar) [17–20] and found during the study that the NiAl(1 1 0) surface is easier to get oxidized than the Ni(1 0 0) surface. (The gas molecules in the UHV chamber consist mainly of H_2 and H_2O, and the oxidation is due to the interaction of the Ni(1 0 0) and Ni(1 1 0) surfaces with H_2O) We therefore believe that the reason why the NiAl(1 1 0) surface is easier to get oxidized than Ni(1 1 0) is the preferential (easier) oxidation of Al metal atoms in the NiAl alloy.

The Standard Electrode Potential is −1.63 V for the reaction $Ti^{4+} + 4e^- \leftrightarrow Ti(s)$ [16], −1.45 V for the reaction $Zr^{4+} + 4e^- \leftrightarrow Zr(s)$ [21], −0.44 V for the reaction $Fe^{2+} + 2e^- \leftrightarrow Fe(s)$ [16], and 0.34 V for the reaction $Cu^{2+} + 2e^- \leftrightarrow Cu(s)$ [22] where (s) represents solid. The Standard Electrode Potential of the reaction forming Al^{3+} ions (−1.66 V) is the lowest, and therefore Al atoms in the as-cast alloy get preferentially oxidized. The experimental observation that the composition of Al metal ions (41.3%) is much higher than the nominal concentration of Al in the alloy (9.5%), therefore, can be mainly attributed to the easier oxidation of Al atoms.

The Standard Electrode Potential of the reaction for formation of Cu^{2+} ions from Cu^0 (0.34 V) is higher and Cu^0 is more difficultly oxidized. So we saw a significantly smaller composition of Cu^{2+} cations (2.85%) than the nominal composition of Cu in the alloy (19.5%). The nominal composition of Ti (5%) is the same as that of Fe. However, we did not detect Fe ions. This can be attributed to the difference in the Standard Electrode Potential of the reactions forming ions of Ti^{4+} and Fe^{2+}. The Standard Electrode Potential of the reaction forming Fe^{2+} ions (−0.44 V) is much higher than that of the reaction forming Ti^{4+} ion (−1.66 V) and Fe atoms are much harder to get oxidized than Ti atoms. Thus, the composition of Fe^{2+} ions can be lower than the detection limit of XPS.

Our preferential oxidation model can be used to explain the experimental observations Qin et al. made [23]. Qin et al. observed in the $Ti_{45}Zr_{10}Pd_{10}Cu_{31}Sn_4$ bulk metallic glass that the composition of Zr^{4+} and Ti^{4+} ions in the film of the as-polished alloy was higher than the nominal composition, and that the Cu^{2+} composition was lower than the nominal composition. No Pd^{2+} ions were detected in the film. The enriched Zr^{4+} and Ti^{4+} ions in the film can be due to the lower Standard Electrode Potential of the reactions forming Zr^{4+} and Ti^{4+} ions. The composition of Cu^{2+} ions smaller than the nominal composition can be attributed to the higher Standard Electrode Potential of the reactions forming Cu^{2+} ions. The Standard Electrode Potential of the reactions forming Pd^{2+} ions (0.915 V) [24] is the highest, which can be responsible for detecting no Pd^{2+} ions in the film.

4.2. Composition changes in the film of NaCl- and HCl-solution immersed metallic glass alloy relative to the as-cast alloy

We can see from Table 1 that the compositions of metal ions in the film of the NaCl immersed alloy are different from those of the as-cast alloy. Such composition change can be explained by reactions (3) and (5) which occur at the film/solution interface. Cl^- ions, which originate from dissociation of NaCl molecules in solution, should play an important role in reactions (3) and (5). To keep reaction (3) going, metal ions in the film are required to transport toward the film/solution interface and to fill in cation vacancies close to the film/solution interface. According to the point defect model [13], when a Cl^- ion can go into a surface oxygen vacancy, cation vacancy/oxygen vacancy pairs are produced in the film via a Schottky-pair type of reaction ($\text{Null} \rightarrow V_M^{\chi'} + (\chi/2)V_{\ddot{O}}$) where $V_M^{\chi'}$ represents a cation vacancy and $V_{\ddot{O}}$ an oxygen vacancy. The oxygen vacancies in turn react with additional Cl^- ions at the film/solution interface to generate yet more cation vacancies. The reaction for production of cation vacancies is autocatalytic. The cation vacancies diffuse toward the alloy/film interface and thus cations (metal ions) can transport to the film/solution interface via the diffusion of cation vacancies. As a result, reaction (3) can continue. To make reaction (5) happen, hydrogen ions (H^+) are required. H^+ ions arise from reaction (4); and in this reaction, water molecules in solution can react with oxygen vacancies (which can be produced by the Schottky-pair type of reaction), producing H^+ ions.

Compared with that of the as-cast alloy, the composition of Al ions in the film of the NaCl solution immersed alloy decreased significantly. This can be attributed to two reasons. First, the radius of Al ions (53.5 pm) is the smallest in the film and the radii of the other ions are 72 pm for Zr^{4+}, 73 pm for Cu^{2+}, and 60.5 pm Ti^{4+} [25]. Al ions can more easily transport in the passive film and arrive at the film/solution interface, thus preferentially getting dissolved into solution via reaction (3). Second, the Al oxide can be easily dissolved in the NaCl solution via reaction (5). Therefore the composition of Al ions in the NaCl solution immersed alloy is lower than in the as-cast alloy.

In water, HCl molecules are dissociated into hydronium ions (H_3O^+) and chloride ions (Cl^-) [26,27] and NaCl molecules into Na^+ and Cl^- ions. The concentration of Cl^- ions in the HCl solution (1 M) is much higher than in the NaCl solution (0.13 M). However, the compositions of metal ions in the film of the HCl solution immersed metallic glass alloy are not significantly different from those of the NaCl solution immersed metallic glass alloy (Table 1), indicating that the concentration of Cl^- ions has no significant effect on the compositions of metal ions in the concentration range of 0.13–1 M. Based on this XPS result, we suggest that the corrosion reactions occurring in our metallic glass samples should not be the pit corrosion but the steady state corrosion. The SEM images (Fig. 6b and c) corroborate this XPS observation. The fact that no pit corrosion occurs can be attributed to the Ti^{4+} ions in the film, based on Tam's observation. Tam investigated the effect of Ti on corrosion behavior in metallic glasses $Cu_{50}Zr_{45-x}Ti_xAl_5$ using SEM and found that the addition of Ti (atom 5%) significantly increases the resistance of pit corrosion [28].

We can see from Table 1 that the composition of Zr ions is dominated in the film of the NaCl- and HCl-solution immersed alloy, indicating that the ZrO_2 oxide in the film is very hard to get corroded in the corrosive solutions. This result is in agreement with the observation of Qin et al. that the good corrosion resistance of the $Ti_{45}Zr_{10}Pd_{10}Cu_{31}Sn_4$ bulk metallic glass can be related to the formation of Ti^{4+} and Zr^{4+} ions in the film [23].

5. Conclusions

We have made four interesting observations. First, the composition of Al metal ions in the film of the as-cast metallic glass (41%) is much higher than the nominal Al composition of the alloy (9.5%). We suggest that this should be attributed to the preferential oxidation of Al atoms. Second, the composition of Al ions in the film of the immersed metallic glass decreases significantly, indicating that the toxic Al oxide and Al ions in the film are dissolved into the solutions during immersion. Third, the concentration of Cl^- ions has no significant effect on the compositions of metal ions in the film. Fourth, the composition of Zr ions dominates in the film of the immersed metallic glass, indicating that the ZrO_2 oxide in the film is very hard to get corroded in the corrosive solutions.

Acknowledgment

This work is financially supported by The Project Sponsored by the Scientific Research Foundation for the Returned Overseas Chinese Scholars, State Education Ministry and the Innovative Project of Central China Normal University. This work also got a financial aid from Natural Science Foundation of Jiangsu Province (No: BK2009724) and Industry R&D Program (No: GY2009003).

References

[1] W. Klement, R.H. Willens, P. Duwez, Nature 187 (1960) 869.
[2] H.S. Chen, D. Turnbull, Acta Metall. 17 (1969) 1021.
[3] H.S. Chen, D. Turnbull, Acta Metall. 22 (1974) 1505.
[4] A. Inoue, T. Zhang, T. Masumoto, Mater. Trans. JIM 30 (1989) 965.
[5] A. Inoue, T. Nakamura, N. Nishiyama, T. Masumoto, Mater. Trans. JIM 33 (1992) 937.
[6] W.H. Wang, C. Dong, C.H. Shek, Mater. Sci. Eng. R 44 (2004) 45.
[7] A. Inoue, Mater. Trans. JIM 36 (1995) 866.
[8] C.J. Gilbert, R.O. Ritchie, W.L. Johnson, Appl. Phys. Lett. 71 (1997) 476.
[9] S.J. Pang, T. Zhang, H. Kimura, K. Asami K, A. Inoue, Mater. Trans. JIM 41 (2000) 1490.
[10] C.L. Qiu, Q. Chen, L. Liu, K.C. Chan, J.X. Zhou, P.P. Chen, S.M. Zhang, Scipta Mater. 55 (2006) 605.
[11] L. Liu, C.L. Qiu, Q. Chen, K.C. Chan, S.M. Zhang, J. Biomed. Mater. Res. A (2007) 160.
[12] L. Liu, Z. Liu, K.C. Chan, H.H. Luo, Q.Z. Cai, S.M. Zhang, Scripta Mater. 258 (2008) 231.
[13] D.D. Macdonald, J. Electrochem. Soc. 139 (1992) 3434.
[14] J.W. Schultze, M.M. Lohrengel, Electrochim. Acta 45 (2000) 2499.
[15] M. Paunovic, M. Schlesinger, Fundamentals of Electrochemical Deposition, Wiley, New York, 1998.
[16] P. Atkins, Physical Chemistry, 6th ed., W.H. Freeman and Company, New York, 1997.
[17] M. Tan, B.V. King, Surf. Sci. 600 (2006) 2771.
[18] M. Tan, B.V. King, Phys. Rev. B 73 (2006) 075414.
[19] M. Tan, Appl. Surf. Sci. 253 (2007) 8905.
[20] M. Tan, B.V. King, Surf. Sci. 602 (2008) 2713.
[21] P. Vanýsek, Handbook of Chemistry and Physics, 88th ed., Chemical Rubber Company, 2007.
[22] A.J. Bard, R. Parsons, J. Jordan, Standard Potentials in Aqueous Solutions, Marcel Dekker, New York, 1985.
[23] C.L. Qin, J.J. Oak, N. Ohtsu, K. Asami, A. Inoue, Acta Mater. 55 (2007) 2057.
[24] A.J. Bard, L.R. Faulkner, Electrochemical Methods. Fundamentals and Applications, 2nd ed., John Wiley and Sons Inc., 2001.
[25] R.D. Shannon, Acta Cryst. A 32 (1976) 751.
[26] R. Perry, D. Green, J. Maloney, Perry's Chemical Engineers' Handbook, 6th ed., McGraw-Hill Book Company, 1984.
[27] D. Lide, CRC Handbook of Chemistry and Physics, 81st ed., CRC Press, 2000.
[28] M.K. Tam, A thesis for the Master degree, Department of Physics and Material Science, City University of Hong Kong, Hong Kong, 2005.